

## 4.5 APPLICATION OF COAMPS<sup>TM</sup> OCEAN DATA ASSIMILATIONS IN THE AOSN II MONTEREY BAY

Xiaodong Hong<sup>1\*</sup>, James Doyle<sup>1</sup>,  
Richard M. Hodur<sup>1</sup>, and Paul J. Martin<sup>2</sup>

<sup>1</sup>Naval Research Laboratory, Monterey, CA 93943

<sup>2</sup>Naval Research Laboratory, Stennis Space Center, MS 39529

### 1. Introduction

The ocean data assimilation component of the Navy's Coupled Ocean/Atmosphere Mesoscale Prediction System (COAMPS<sup>TM</sup>) (Hodur 1997) includes a three-dimensional Multivariate Optimum Interpolation (MVOI) ocean analysis, a hydrostatic ocean forecast model, and a flux-coupler for obtaining surface forcing from the atmospheric model. The ocean model used in COAMPS is the NRL Coastal Ocean Model (NCOM) (Martin, 2000). Preliminary studies have been conducted using COAMPS and NCOM with two-way interactive coupling (Pullen et al. 2004). In this study, we use one-way coupling with the COAMPS atmospheric forecast model. The COAMPS surface forecast fields are used to drive the NCOM forecast. The observations used in the ocean MVOI analysis are obtained from the Global Ocean Data Assimilation Experiment (GODAE) server at the Fleet Numerical Meteorology and Oceanography Center (FNMOC). In addition, data obtained by the Autonomous Ocean Sampling Network II (AOSN II) Monterey Bay field experiment from August 3 to September 8, 2003 were also assimilated in this study. The COAMPS ocean data assimilation system was applied to the Monterey Bay area to validate the coupled assimilation system and to investigate the circulation and coastal upwelling in this area.

### 2. System Setup

The COAMPS ocean data assimilation system uses a sequential incremental update cycle and the ocean model forecast fields are used to provide background values. A three-dimensional MVOI ocean analysis is performed every 24 hours to obtain the increment fields for updating the

ocean model forecast. The computational domain for NCOM covers both the Monterey and San Francisco Bay areas. The horizontal grid spacing is 3 km and vertical resolution ranges from 2 to 536 m with 40 levels. The ocean model forecast uses the 1/8° global NCOM real-time nowcast/forecast fields - (Fig. 1) for initial and lateral boundary conditions. The lateral boundary conditions for regional NCOM are updated every 3 hours.

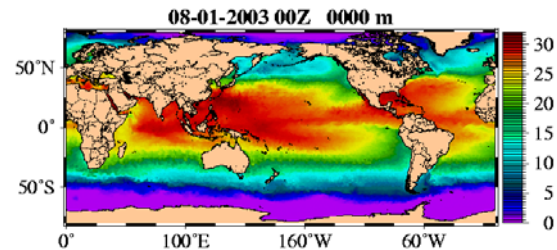


Fig. 1. Global NCOM sea surface temperature.

The surface air-sea fluxes for the ocean model were obtained from the real-time AOSN II COAMPS atmospheric forecasts. These forecasts are produced twice daily out to 72 h on a quadruple-nested grid system with horizontal resolutions of 81, 27, 9, and 3 km. The COAMPS inner-most mesh (3-km resolution) hourly surface variables were used to force NCOM. Surface latent and sensible heat flux were computed using the wind speed, air temperature, and humidity from the atmospheric model, the predicted sea surface temperature from the ocean model, and standard bulk formulas with the Kondo (1975) drag coefficient. This interactive flux calculation provides feedback from the ocean model (Castellari et al. 2000). The high-resolution COAMPS winds provide a good representation of the narrow bands (about 10 by 50 km) of strong wind stress and wind stress curl parallel to the coast and adjacent to major California coastal promontories (Pickett and Paduan 2003). Observations of sea surface temperature from satellites have shown that cold-water plumes off northern California were anchored to coastal topography (Kelly 1985).

---

\* Corresponding author address: Xiaodong Hong,  
Naval Research Laboratory, Monterey, CA 93943;  
e-mail: hong@nrlmry.navy.mil.

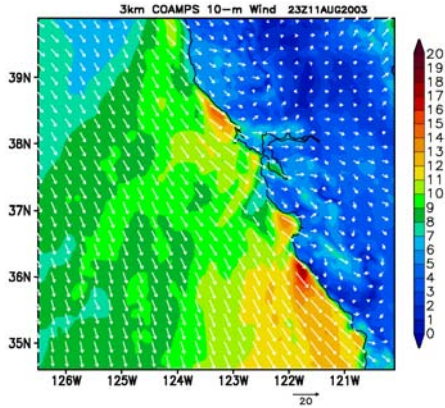


Fig. 2. COAMPS 10-m wind speed from grid 4.

### 3. Data

Data from the GODAE server and AOSN II observations were used in the system. The GODAE data include altimeter, ship, profile, MCSST, and SSM/I observations (Fig. 3). The AOSN II data used here include NPS aircraft SSTs and data from moorings m1 and m2.

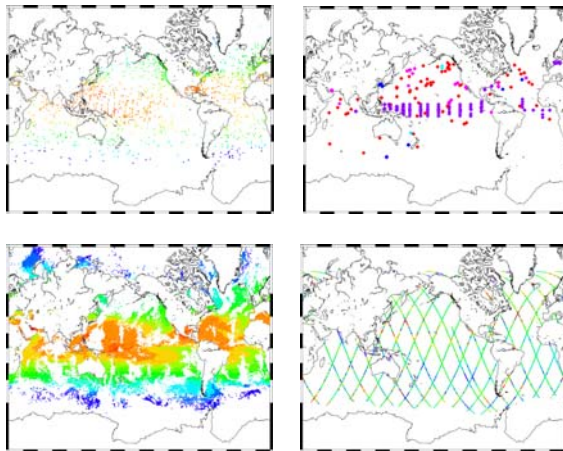


Fig. 3. Data from GODAE server includes altimeter, ship, profile, MCSST, and SSM/I at FNMOC.

All data are quality controlled before entering the data assimilation system. The quality control includes sensibility checks, gross error checks, and consistency checks, which are performed prior to the analysis.

Five ocean variables including temperature, salinity, geopotential, and u-v velocity components are simultaneously analyzed with the ocean model forecast fields used as background values. Three-dimensional MVOI incremental fields from the analysis are used to update the model restart fields.

### 4. Upwelling/Relaxation

The upwelling/relaxation features during the AOSN II experiment in August 2003 are explored using the results from the simulation. At this time, the winds over Monterey Bay can be described as having periods that are upwelling favorable or unfavorable as shown in Fig. 4. The regional circulation corresponds to two distinct hydrographic states: an upwelling state and a relaxation state. The winds in early August were not favorable for upwelling. From August 7 to 19, the prevailing north/northwesterly winds (i.e., directed towards the south/southeast) are re-established and induce upwelling. Warmer surface waters are forced offshore, allowing cold, nutrient-rich waters to rise to the surface near the coast. From August 20 to 24, the winds were light with a south or southwest direction, resulting in relaxation conditions. During this period, upwelling along the coast diminished and the warm offshore water moved shoreward. During the latter portion of August, the wind forcing again became upwelling favorable.

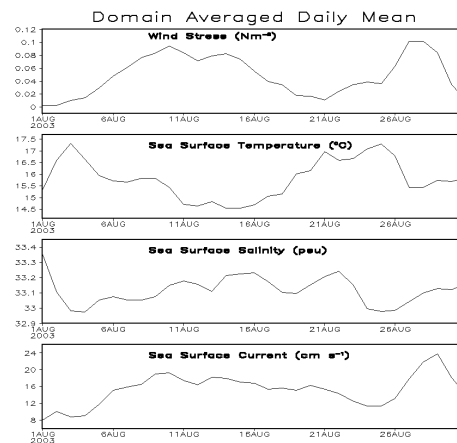


Fig. 4. Domain averaged daily wind stress, sea surface temperature, salinity and current.

During the upwelling period from 7 to 19 August, two upwelling centers resulted from the substantial upwelling off Point Ano Nuevo and Point Sur. Figure 5 shows the sea surface temperature forecast for 18 h (valid at 18Z Aug. 15, 2003) using the assimilation of observed data (GODAE, aircraft SST, moorings m1 and m2). The assimilation realistically depicts the signature of the upwelling since it had been proceeding for several days. Large horizontal surface temperature gradients occurred between the upwelled cold water and the offshore warm water.

A cold tongue of upwelled water off Point Ano Nuevo was advected southward across the mouth of Monterey Bay. The plume of upwelled cold water extended southward and joined with the upwelled cold water from Point Sur, resulting in a large cold water region located just off the coast. Upwelled cold water also may have advected seaward as suggested in a previous observational study (Rosenfeld et al. 1994).

The NCOM sea surface temperature forecasts were compared with satellite observations of sea surface temperature (Fig. 6). These experimental AVHRR SST data were not used in the data assimilation experiments. The basic observed features are captured by the NCOM forecasts. These include (1) strong upwelling that occurred off Point Ano Nuevo and Point Sur; (2) upwelled water that was advected southward across the mouth of Monterey Bay and joined with cold water from Point Sur; and (3) warmer offshore water that was advected toward the mouth of Monterey Bay.

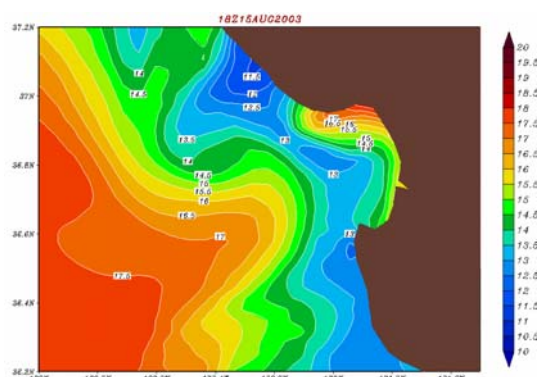


Fig. 5. Sea surface temperature from 18 h forecast valid at 18Z Aug. 15, 2003.

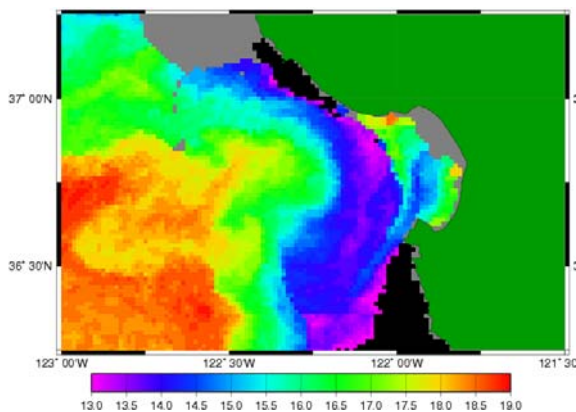


Fig. 6. Experimental AVHRR SST at 1858Z Aug. 15, 2003. (NOAA POES AVHRR, Courtesy NWS and NOAA Coastwatch)

Figure 7 shows a vertical cross section of forecast temperature along 37.05 °N at 18Z Aug. 15, 2003. The isopleths of temperature are sloped upward towards the coast, indicating that the upper-layer warm water was pushed offshore and deep cold water was brought to the surface by Ekman transport and pumping (Pickett and Paduan, 2003). An upwelling front exists between the upwelled and offshore water with a characteristic gradients of 5°C per 100 km across the front.

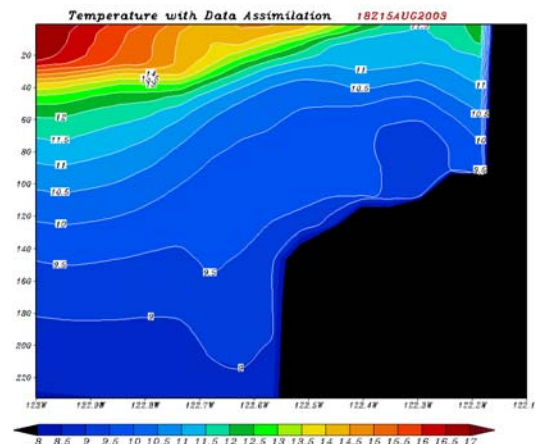


Fig. 7. Vertical cross section of temperature along 37.05 °N on 18 Z Aug. 15, 2003.

During the relaxation period, an anti-cyclonic meander within the California current moved coastward and cold upwelled water was replaced by warm offshore water. Fig. 8 indicates that warm water occupied the coastal region with temperatures of about 16 °C at the surface. Since there were no aircraft SSTs available for assimilation on Aug. 23 and 24, this relaxation

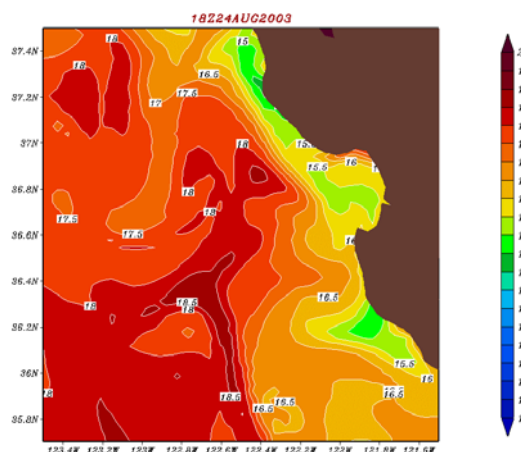


Fig. 8. Sea surface temperature from 18 h forecast valid at 18Z Aug. 24, 2003.



episode was most likely a model response to the atmospheric forcing. Cold water still existed in the upwelling center, however, the areal extent was considerably reduced as can be seen from the model forecast (Fig. 8) and from the AVHRR SSTs (Fig. 9).

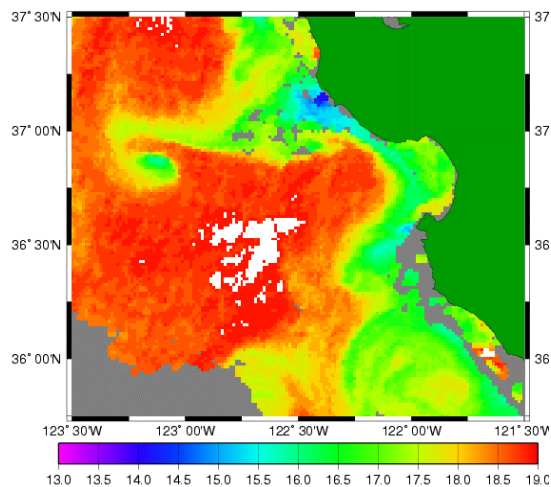


Fig. 9. Experimental AVHRR SST at 1856Z Aug. 24, 2003. (NOAA POES AVHRR, Courtesy NWS and NOAA Coastwatch)

The isopleths of temperature slope downward towards the coast during the relaxation stage (Fig. 10), indicating that the offshore warm water was advected to the nearshore. Downwelling forced the upper-layer water downward following the slope of the topography. The upwelling front is located near the coast. Warm water recapped the surface layer in the original upwelling area. There still exist smaller temperature gradients across the front with about a 2.0 °C difference.

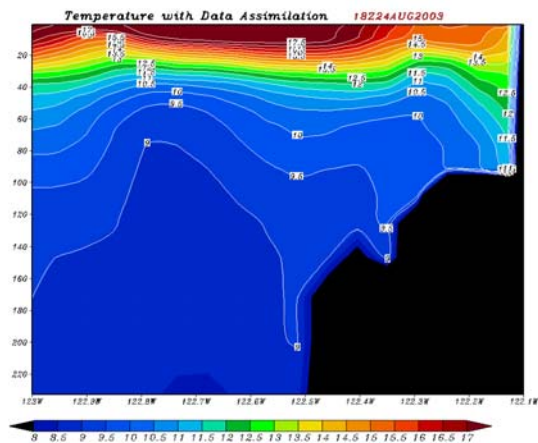


Fig. 10. Vertical cross section of temperature along 37.0 °N on 18 Z Aug. 15, 2003.

Significant diurnal fluctuations in upwelling occurred during the simulation (Fig. 11) associated with diurnal fluctuations in the surface atmospheric conditions. Large surface heating differences between the Central Valley and the coastal marine atmosphere resemble a classic sea-breeze circulation (Banta et al. 1993). In Fig. 11, the simulated sea surface temperature decreased and the salinity increased during the upwelling period and vice versa during the relaxation period. The diurnal fluctuations for wind stress, surface temperature, and salinity are superimposed on the longer period changes associated with the upwelling and relaxation events. The peak upwelling occurred on Aug. 16.

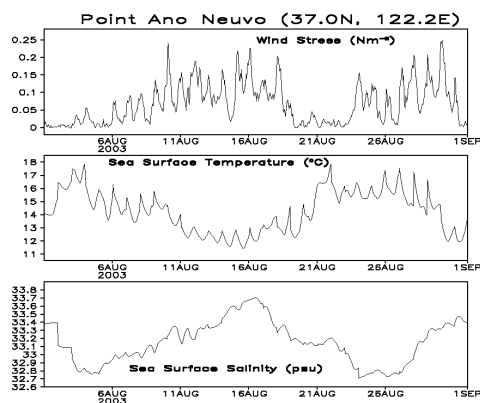


Fig. 11. Time series of surface wind stress, temperature and salinity at Point Ano Nuevo.

## 5. Verification

Besides comparing the NCOM forecast with the experimental AVHRR SSTs as shown above in Fig. 6 and 9, the NCOM forecast surface current was also compared with the NPS mean HF radar surface currents (averaged over a 25-h period). Neither the AVHRR SSTs nor the HF radar surface current data were used in the model data assimilation.

The mean surface temperature and current from the NCOM forecast were computed for the same time period as the HF radar surface current. Figures 12 and 13 depict mean values from 5Z Aug. 15 to 6Z Aug. 16 2003. The model shows that cold, upwelled water from Point Ano Nuevo was advected across and into the mouth of Monterey Bay and joined with cold water off Point Sur south of Monterey Bay. Both the model and the HF radar show a cyclonic circulation in the bay. However, the size of the cyclonic circulation is smaller in the model and its location is confined

within the northern part of the bay. This may be caused by the stronger southeastward current in the model simulation that advected cold water into the southern part of Monterey Bay. The model results show the warm water offshore in the area of anti-cyclonic circulation to be advected further to the south and closer to the bay. The larger area of cold water in the southern part of Monterey Bay and the stronger warm offshore meander could be due to insufficient model resolution. Future work with the AOSN II will use a higher-resolution nested grid in the Monterey Bay area.

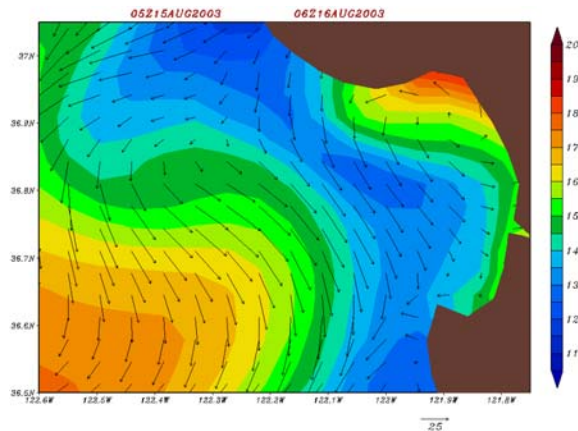


Fig. 12. 25 h mean NCOM surface temperature and current from 5Z, 15 Aug. to 6Z, 16 Aug. 2003.

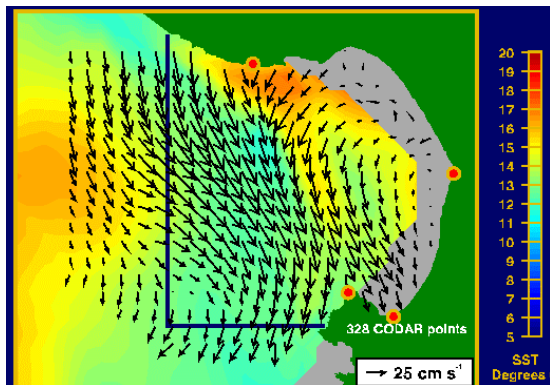


Fig. 13. 25 h mean HF radar surface current from 5Z 15 Aug. to 6Z 16 Aug. 2003. (Courtesy of Jeff Paduan, Naval Postgraduate School)

The mean NCOM forecast for a relaxed state (Fig. 14) is also compared to the mean HF radar observation at this time (Fig. 15). Both show slightly colder water in the southern part of the bay, a cyclonic circulation inside the bay, and an anti-cyclonic circulation outside the bay. The size and strength of these two circulations are similar in the HF radar analysis. However, the forecast model shows a smaller current speed for the

cyclonic circulation inside the bay than for the anti-cyclonic circulation outside the bay. This again could be a result of the coarse horizontal resolution used in the model. The HF radar can provide significant detail of the surface current in Monterey Bay, and in the future, these current data will be used in the assimilation.

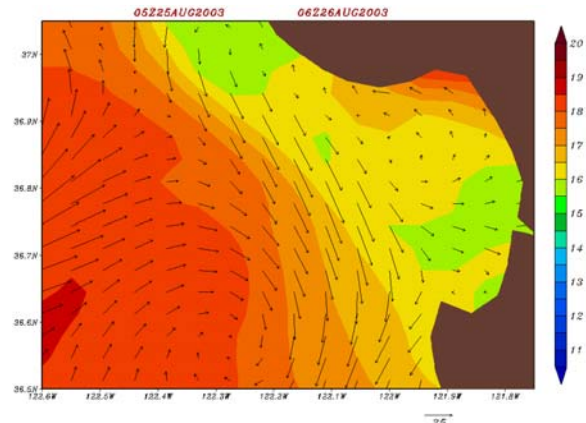


Fig. 14. 25 h mean NCOM surface temperature and current from 5Z, 25 Aug. to 6Z, 26 Aug. 2003.

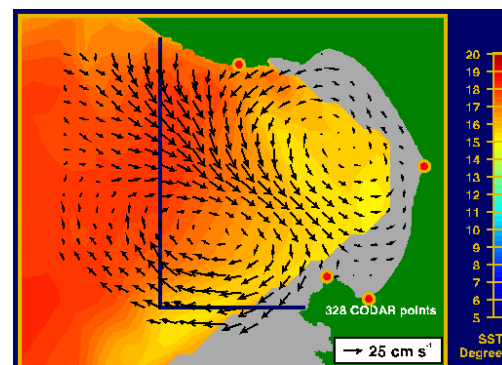


Fig. 15. 25 h mean HF radar surface current from 5Z, 25 Aug. to 6Z, 26 Aug. 2003. (Courtesy of Jeff Paduan, Naval Postgraduate School)

## 6. Summary

The relocatable ocean data assimilation system in COAMPS was applied to the AOSN II field experiment in Monterey Bay. The ocean forecast used hourly atmospheric forcing from COAMPS and 3-hourly lateral boundary conditions from Global NCOM. These lateral boundary conditions enabled the regional model to have proper large-scale forcing through its open boundaries. Assimilated data from the systems' default database (the GODAE server) provided large-scale observed features for the model forecast. High-density AOSN II data in Monterey Bay were also assimilated to provide information about

smaller-scale features. The simulated upwelling, upwelling transport, and diurnal changes in Monterey Bay were compared with the experimental AVHRR SSTs and with temporally-averaged HF radar surface currents. Both of these observations were independent of the model assimilation. The model results compared well with the observations. However, higher horizontal resolution will be necessary for the simulation of smaller-scale features in future applications of this system.

upwelling center: a cold water source for Monterey Bay. *Cont. Shelf Res.*, 14, 931-964.

## 7. References

- Banta, R. M., L. D. Olivier, and D. H. Levinson, 1993: Evolution of the Monterey Bay sea-breeze layer as observed by pulsed Doppler lidar. *J. Atmos. Sci.*, 50, 3959-3982.
- Castellari, S., N., Pinardi, and K. Leaman, 2000: Simulation of water mass formation processes in the Mediterranean Sea: influence of the time frequency of the atmospheric forcing. *J. Geophys. Res.*, 105, C10, 24157-24181.
- Hodur, R. M., 1997: The Naval Research Laboratory's Coupled Ocean/Atmosphere Mesoscale Prediction System (COAMPS). *Mon. Wea. Rev.*, 125, 1414-1430.
- Kelly, K. A., 1985: The influence of winds and topography on the sea surface temperature patterns over the northern California slope. *J. Geophys. Res.*, 90, 11783-11798.
- Kondo, J., 1975: Air-sea bulk transfer coefficients in diabatic conditions. *Boundary-Layer Met.*, 9, 91-112.
- Martin, J. P., 2000. Description of the Navy Coastal Ocean Model Version 1.0. Naval Research Laboratory, *NRL/FR/7322—00-9962*, pp. 1-42.
- Pickett, M. H. and J. D. Paduan, 2003: Ekman transport and pumping in the California Current based on the U.S. Navy's high-resolution atmospheric model (COAMPS), *J. Geophys. Res.*, 108, C10, 3327-3337.
- Pullen, J., James Doyle and Richard Signell, 2004: Adriatic Air-Sea Coupling. (to be submitted to *Mon. Weather. Rev.*).
- Rosenfeld, L. K., Schwing, F. B., Garfield, N., Tracy, D. E., 1994: Bifurcated flow from an